

KASDI MERBAH- OUARGLA UNIVERSITY
FACULTY OF HYDROCARBONS, RENEWABLE ENERGIES AND EARTH
AND UNIVERSE SCIENCES
DEPARTMENT OF EARTH AND UNIVERSE SCIENCE



Academic Master Thesis
Field: Earth and Universe Sciences
Sector: Geology
THEME

**Contribution of High resolution remote sensing to
lineaments mapping of the "Tesnou" region
Western hoggar**

Presented by:

MRIGA MOUNA

In front of the jury:

President: Nawal Maabdi

MCB Univ. Ouargla

Supervisor: Dr. Hammad Nabila

MCB Univ. Ouargla

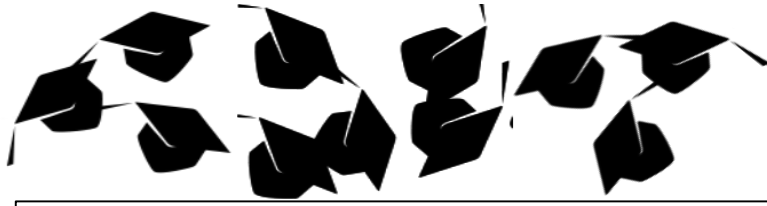
Co-supervisor: Sahri Nassira

MCB Univ. Ouargla

Examiner : Hamza Laouini

MCB Univ. Ouargla

University year: 2022/2023.



DEDICATIONS

Finally, this day has arrived , it was a very difficult academic year at all levels . That is why I dedicate this work to my family, who supported me throughout my mom's and dad's careers. They didn't give me any material or moral things.

My second mother accompanied me with her care and interest. My second father, who always motivated me and encouraged me to ask for science.

To my professor who accompanied me by whipping and then my mom's girlfriend who was gifted to me by the university,

To my best friends, especially Iman and Safa, and to everyone who supported me during my school career from near or far. to every one i love....thank you



APPRECIATION AND GRATITUDE

I thank Allah who supported me and inspired me and sarcastically for all the reasons that helped me to reach my goals. I thank my framed professor and all the professors who studied me during my course of study at the primary, intermediate high school and university . Thank you all



الملخص:

يعرض هذا العمل نتائج الاستخراج اليدوي و التلقائي للخطوط في منطقة تسنو الواقعة غرب الهقار. يتم استخراج هذه الخطوط عن طريق الإستشعار عن بعد بمجموعة من عملياته وبرنامج سوفر. تم استخدام صور القمر الصناعي لاندسات 8 خضعت هذه البيانات إلى مراجعة ببرنامج سناب وللتحقق من صحة النتائج بالخريطة الجيولوجية الخاصة بالمنطقة.

الكلمات المفتاحية: الاستشعار عن بعد ، لاندسات 8 ، الاستخراج اليدوي للخطوط ، الخريطة الجيولوجية

Résumé :

Ce travail montre les résultats de l'extraction manuelle et automatique des linéaments dans la région de Tesnou de l'ouest du Hoggar. Ces linéaments sont extraits par approche de télédétection photo interprétative sous Surfer. Ces approches sont basées des traitements comme les filtres directionnels, l'ACP et les compositions colorées appliquées à l'image de LANDSAT 8 OLI. Ces données ont été traité sous SNAP et à une vérification de ces résultats via la comparaison à la carte géologique.

Mots-clés : télédétection, landsat 8 oli, l'extraction manuelle des linéaments, cartes géologique.

Abstract :

This work shows the results of manual And automatic extraction of the lineaments in the Tsnou region of the west of Hoggar. These lineaments are extracted by photointerpretative remote sensing approach and Surfer program. This approaches is based first on a set of treatments and processing such directional filter, ACP. These data have been processed on Snapp and a verification of the results were compared via the geological map.

Keywords: remote sensing, landsat8 oli, manual extraction of the lines, geological maps.

Table of content

Didicas	I
Appreciation and gratitude	II
Abstract	III
Table of content	V
Liste of tables	VII
Liste of Illustrations	VI
General introduction	2
Chapter 1 Regional and local geological framework	
1/Geographical location of el hoggar:	4
2. Geological framework of the study area:	5
2.1. Stratigraphy:	6
2.1.1. Volcano-sedimentary series:	6
2.1.2. Lower base (volcano-sedimentary):	7
2.1.3. Medium base (terrigenous):	7
2.2. Magmatism:	7
The Afedafeda-type preorogenic magmatic complex (Tin tekadiouit-taklet):	7
The Aderniba type synorogenic magmatic complex (Imezzarene):	8
The Taourirt-type post-orogenic magmatic complex:	8
2.3. Tectonics	8
Chapter 2 Materials and methods	
Materials	10
Data sets used	10
Geoscientific data:	11
2/Software:	11
SNAP system:	11
Surfer system:	11
Methodology:	12
Processing Parameters	12
Source bands	12
Compute Rayleigh optical thickness bands	12
Compute bottom of Rayleigh reflectance bands	12
Compute gaseous absorption corrected TOA reflectance bands	12
Compute TOA reflectance bands	12
Add air mass	12
Image resolution in m in target product (S2 MSI only):	12
Sea level pressure in hPa (S2 MSI only)	12
2.1.1. Color composition:	13
Thematic treatment:	15

Didicas	I
Appreciation and gratitude	II
Transformation treatments:	15
Principal component analysis (PCA):	15
Advantages of PCA:	15
band Ratio	17
Spatial filtering of images:	18
Directional filter:	19
Extraction of lineament	20
Chapter 3 results and discussion	
Results	22
Results of satellite image interpretation analysis	22
Colored composition using Landsat 8 (R7 G3 B2)	22
Colored composition (R7 G6 B1)	22
Enhanced Filter Result:	23
Principal Component Analysis Result (PCA):	23
Band Ratio Result	24
Lineament Mapping .	24
Filtering Treatment Results	24
. Results of manual line extraction:	25
AUTOMATIC EXTRACTION OF LINEAMENTS	26
discussion	27
General Conclusion	29
Bibliography	32

Liste of tables :

Table 1: Band characteristics of "LANDSAT_8 OLI	10
Table 2: Correlations between bands	14
Table 3 : Spatial filter operators (Caloz & Collet, 2001) : The table shows the main types	19

Liste of Illustrations :

01	Figure1: Regional Geographical location of EL hoggar	4
02	Figure 2 : Local Geographical location of the studied area – western hoggar	4
03	Figure 3. Simplified geologic map of the Tuareg Shield (modified from Bertrand and Caby, 1977; Black et al., 1994; Liégeois et al., 1994, 1998, 2003 in Bouzid et al, 2015).	5
04	Figure 4: Modeled 3D cross-section of Iskel terrane thrusting the LATEA metacraton (Azzouni-Sekkal et al., 2003)	6
05	Figure 5: Geological formations in the study area	7
06	Figure: satellite image of tesnou	10
07	Figure: sea level pressure on March 2023	13
08	Figure: for ozone in DUZ	13
09	Figure: tesnou coordinates using colored composition	14
10	Figure: colored composition (R7 G5 B1)	15
11	Figure: pc file of tesnou	16
12	Figure: CP 1	17
13	Figure: CP 2	17
14	Figure: directional filter on (R8 G6 B4) at 90° with 5x5 Kernel	20
15	Figure: extraction Map of the lineaments using DF 135° M 7x7 and geological map	20
16	Figure: Colored composition (R7 G3 B2)	22
17	Figure: Colored composition (R7 G6 B1)	22
18	Figure: Enhanced filter on LANDSAT OLI 861 in RGB	23
19	Figure: Colored composition using PCA (RCP3 GCP2 BCP1)	23
20	Figure : Colored composition using band ratio (R8/6 G2 B1)	24
21	Figure: Directional Filter 135 ° with 7x7 Matrix.	25
22	Figure 39: Map of the lineaments extracted using DF 135° M 7x7 and geological map	25
23	Figure: results of extraction automatic	26
24	Figure: tesnou coordinates using colored composition	27



General introduction

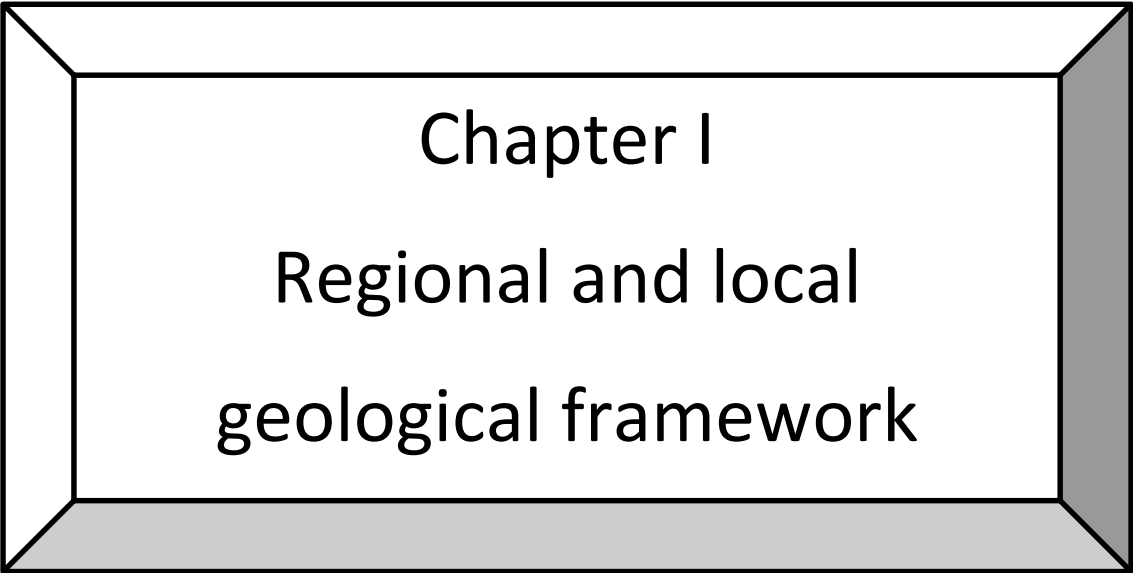
General introduction

The Hoggar represents the central part of the Targhi Shield which extends to the southwest by the Adrar de Evoras Mali and southeast by the Air Niger and consists of an agreed diversity of rocks mainly from the Precambrian period. The Hoggar covers an area of about 550,000 square kilometres. Its economic capital is Tamanrasset. The large area, the diversity of geological formations, and the excellent quality of the outcrops make Hoggar a unique world for geological research. Among its many regions, we chose in this study the Tesnou region located west of the Hoggar, as is the case with any area on the surface of the earth that is subject to changes and distortions on the surface of the earth, and in order to identify accidents, we will study by remote sensing. By extracting lines manually and automatically to obtain linear maps. within the framework of the so-called lineamentary mapping. The term lineament comes from the Latin *linea* which means line. As simple as it seems, it is not easy to define. Many definitions have been given but The best of these, in our opinion, is that given by Hobbs (1912, in O'Leary et al. 1976, Lachaine, 1999): Significant lines of the landscape revealing hidden architecture This definition gives special meaning to the word lineament and associated it with a geological character bearing information on structures. In our short-time study We will try to reach a linear map of the Tesnou region to discover the lines in it through three seasons:

The first chapter: the regional and local geological framework in which we will present the general context of the study area and its and tectonic events.

The second chapter: materials and methods, in which we will discuss all the materials used in the study and the methodology used to follow the steps to address the problem at hand.

Chapter Three: Results, Discussion and Verification In this chapter we will discuss the results obtained through our study of the region using the approach followed. Will this prove that our hypotheses are true or false?



Chapter I

Regional and local
geological framework

1/Geographical location of el hoggar:

The Hoggar or (Ahaggar) is located in the south of the Algerian Sahara with an area of 550,000 km², is located 2,000 km south of Algiers. Its capital economic Tamanrasset has the following coordinates: longitude 5°27', bearing 22°41'.

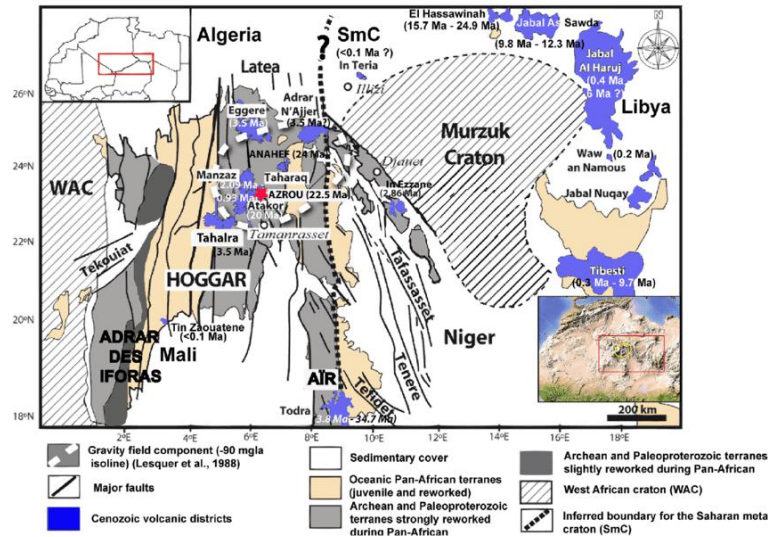


Figure 1: Regional Geographical location of EL hoggar

EL Hoggar is divided into three regions (figure 2): W Hoggar, Central Hoggar, Oriental Hoggar and this study it will be about the western part.

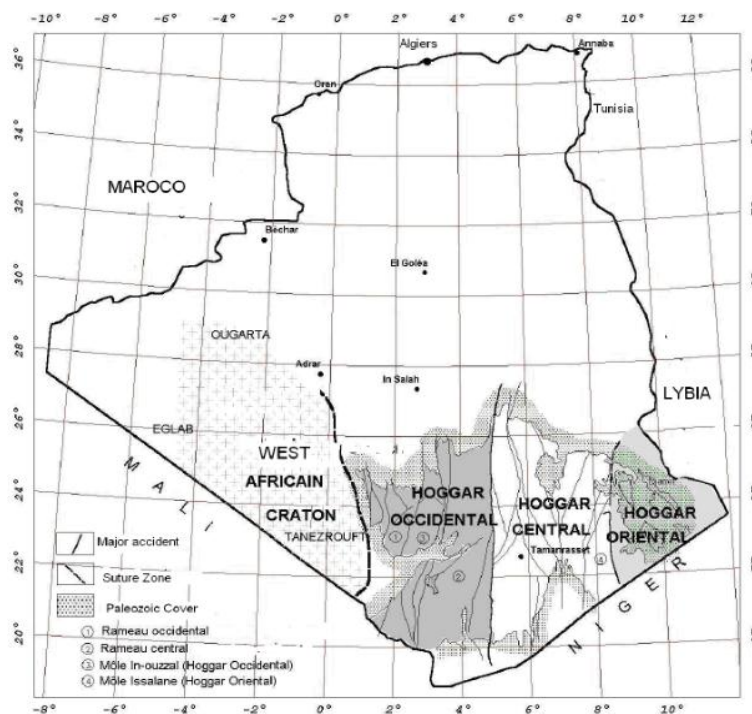


Figure 2 : Local Geographical location of the studied area – western hoggar

The Tuareg Shield consists in fact of 23 distinct geological regions that have collided and shifted along vertical shear zones (Liégeois et al. 2003). These regions were ultimately compressed between the West African craton on the west and the Saharan metacraton on the east (fig. 3). The geological history of each region varies, with some containing Archaean and Palaeoproterozoic blocks that were modified during the Pan-African orogeny. Metacratons, which are cratons partially affected by orogeny while retaining some of their original characteristics, such as the Ouzzal and LATEA metacratons, are present. Some terranes in the Tuareg Shield were formed by the amalgamation of Neoproterozoic oceanic or continental active margins with cratons or metacratons through welding or thrusting processes. This amalgamation primarily occurred between 620 and 580 million years ago, with earlier episodes at 870-850 million years ago and 730-680 million years ago (Caby and Andreopoulos-Renaud, 1987; Caby et al., 1989; Liégeois et al., 1994, Liégeois et al., 2003, Azzouni-Sekkal et al., 2003).

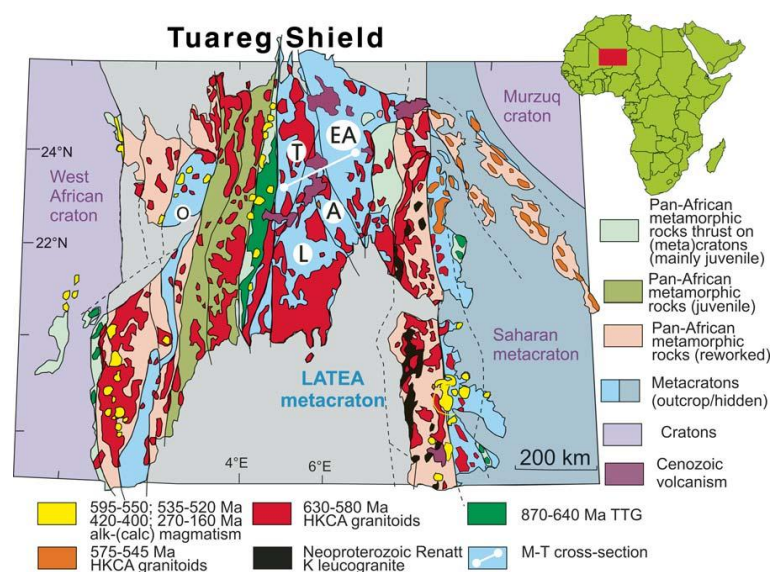


Figure 3. Simplified geologic map of the Tuareg Shield (modified from Bertrand and Caby, 1977; Black et al., 1994; Liégeois et al., 1994, 1998, 2003 in Bouzid et al, 2015).

2. Geological framework of the study area:

The study area, known as "Tesnou," is situated in the western part of the Hoggar region. It is bounded by longitudes 4° E and 5° E, and latitudes 24° and 25° North.

The Iskel terrane, where Tesnou region belongs to, is situated between two distinct geological regions. To the west lies the Neoproterozoic In-Tedeïni terrane, while to the east lies the LATEA microcontinent, ranging from Archean to Neoproterozoic age. It extends approximately 700 km in a north-south direction and has an average width of 60 km. According to Liégeois et al. (2003), the Iskel terrane consists of Neoproterozoic metavolcano-sedimentary deposits that are attributed to various island arc assemblages of different ages.

The eastern boundary of the Iskel terrane is defined by the submeridian fault line at 4°50', marking the western limit of the LATEA. On the western side, the major fault at 4°30' serves as its

boundary (Liégeois et al., 2000). In terms of geological features, the Iskel terrane predominantly exhibits volcano-sedimentary platform deposits, along with serpentinized basic and ultra-basic rock sills. Additionally, there are calc-alkaline granitoids, represented by extensive batholiths of quartz diorite, granodiorite, and occasionally calc-alkaline potassic granites. These granitoids have been dated using the U/Pb method on zircon, with one being dated to around 868 million years ago (Tin-Tékadiouit tonalite) and the other at approximately 839 million years ago (Taklet granite) (Caby et al., 1982).

The Iskel terrane overlaps with the LATEA metacraton and lacks its own mantle lithospheric layer (Liégeois et al., 2000). Figure 4 provides a visual representation of these geological relationships.

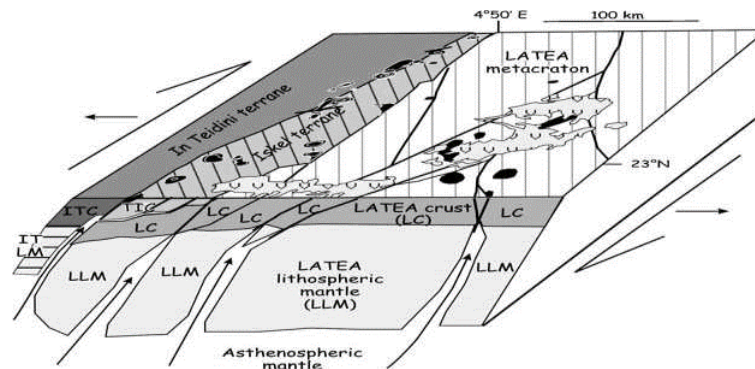


Figure 4: Modeled 3D cross-section of Iskel terrane thrusting the LATEA metacraton (Azzouni-Sekkal et al., 2003)

2.1. Stratigraphy:

2.1.1. Volcano-sedimentary series:

The volcano-sedimentary series in the study area appears as elongated fragments and is bounded by the 4°50' lineament to the east and the 4°30' lineament to the west. This series primarily consists of metamorphosed sediments such as metapelites, metagres, metaquartzites, marbles, metagravellites, intraformational microconglomerates, and breccias. These rocks have undergone low-grade metamorphism, specifically belonging to the green shale facies type.

Within the study area, the volcano-sedimentary series can be further subdivided into two distinct layers.

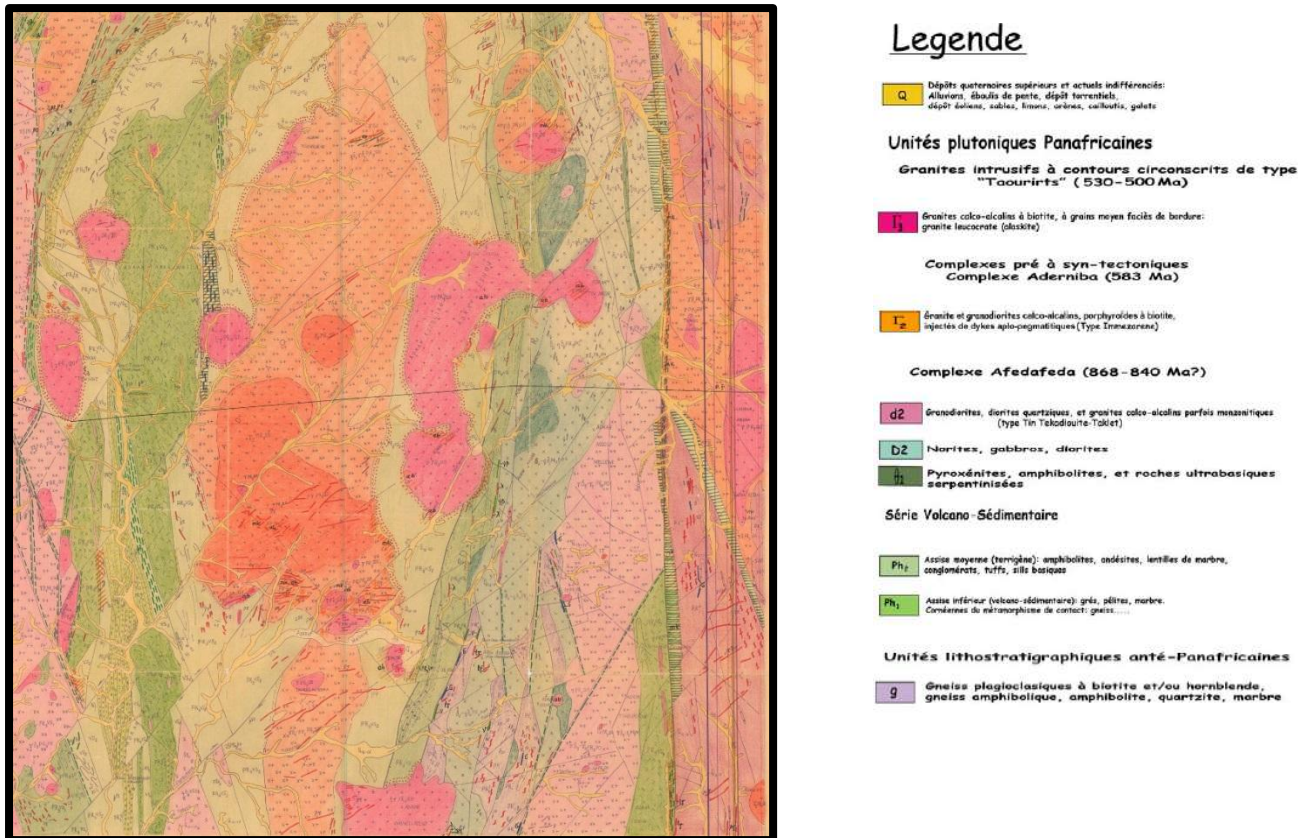


Figure 5: Geological formations in the study area

2.1.2. Lower base (volcano-sedimentary):

It is attached to the Pharusian I cycle (~900-840 Ma), composed of marbles, limestones marly less often dolomitized, meta-sandstone, meta-pelites, meta-aleurolites, passes little powerful quartzites, lenses of intraformal conglomerates, meta-basalts, meta-andesites, tuffs of mixed composition (Blinikov et al., 1991).

2.1.3. Medium base (terrigenous):

Also known as the Pharusian II cycle (800-650Ma) (Blinikov et al., 1991), it is represented by limestone beds and shales, tuffaceous meta-sandstones, meta-aleurolites tuffaceous: meta-pelites, lenses of intraformational conglomerates (Blinikov et al., 1991).

2.2. Magmatism:

The region is characterized by Pan-African age magmatism, which covers over 50% of the area. This magmatism can be divided into three major magmatic complexes, as described by Blinikov et al. (1991) and ORGM (2004):

2.2.1. The Afedafeda-type preorogenic magmatic complex (Tin tekadiouit-taklet):

This complex is a large batholith stretching over more than 600 km in a submeridian direction, from the southern border with Mali to the Tassili region in the north (Caby et al., 1982). It exhibits a

poorly differentiated calc-alkaline character, with a range of compositions from more mafic to more acidic. The contacts between these magmatic rocks and the surrounding host rocks can be intrusive, concordant, or tectonic in nature. Gold-bearing quartz veins are primarily found at the western edge of this intrusion, where basic and intermediate compositions are abundant, and the ferromagnesian minerals are extensively chloritized (A. Semiani et al., 2004).

2.2.2 The Aderniba type synorogenic magmatic complex (Imezzarene):

This orogenic complex displays a calc-alkaline affinity according to Blinikov et al. (1991) and intersects with the Neoproterozoic formations, resulting in contact metamorphism characterized by the development of minerals such as cordierite, sillimanite, and garnet. In the study area, mafic compositions are the most prevalent and include pyroxenites, gabbros, and gabbro-diorites (Blinikov et al., 1991).

2.2.3. The Taourirt-type post-orogenic magmatic complex:

These are confined massifs that exhibit clear boundaries with the surrounding metamorphic and granitic rocks. These magmatic complexes are notable for their distinctive structures and arrangements in concentric rings. Their location appears to be influenced by the presence of the major submeridian strike-slip fault at 4°50' (Blinikov et al., 1991).

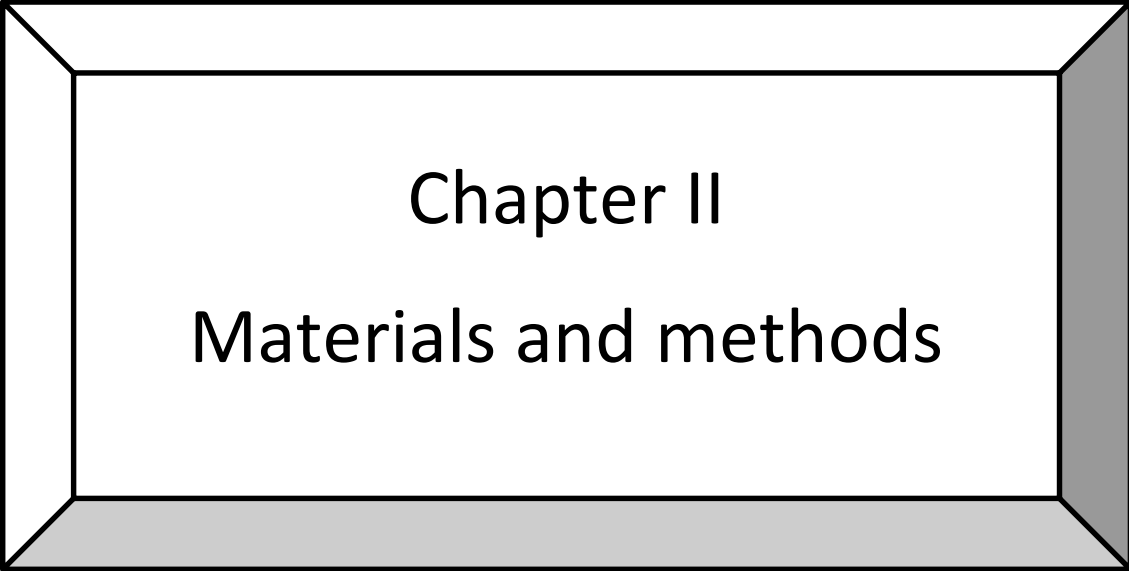
2.3. Tectonics

The tectonic history of the Tesnou region is characterized by two major phases (Blinikov et al., 1991):

Ductile tectonics corresponding to a compressive episode that affected all formations in the Hoggar region. This phase resulted in:

- Development of tight isoclinal folds with overturned limbs and sub-horizontal axes.
 - Emplacement of syntectonic granitic intrusions, such as the Afedaféda-Tintekadiouite Taklet, controlled by N30° right-lateral strike-slip faults (NNW-SSE orientation).
2. Contact metamorphism with garnet, disthene, and sillimanite:
- The final deformation phase involved transcurrent shearing along submeridian mylonitic shear zones.
 - Associated features include tightly folded structures oriented north-south.
 - Right-lateral strike-slip faults (NNE-SSW orientation) were formed.
 - Late reactivation of submeridian faults accompanied the development of vertically-oriented folds.
 - Late to post-orogenic granites, known as the "Taourirt," were emplaced.

The post-Pan-African tectonics in the region is characterized by NE-SW and EW-trending faults, which crosscut the Pan-African structures and faults distinctly.



Chapter II

Materials and methods

Materials:**1/data sets used**

The data used in our study consist of LANDSAT_SCENE_ID = "LC81930432023106LGN00" acquired by "LANDSAT_8 SPACECRAFT on 16/04/2023 (fig.).

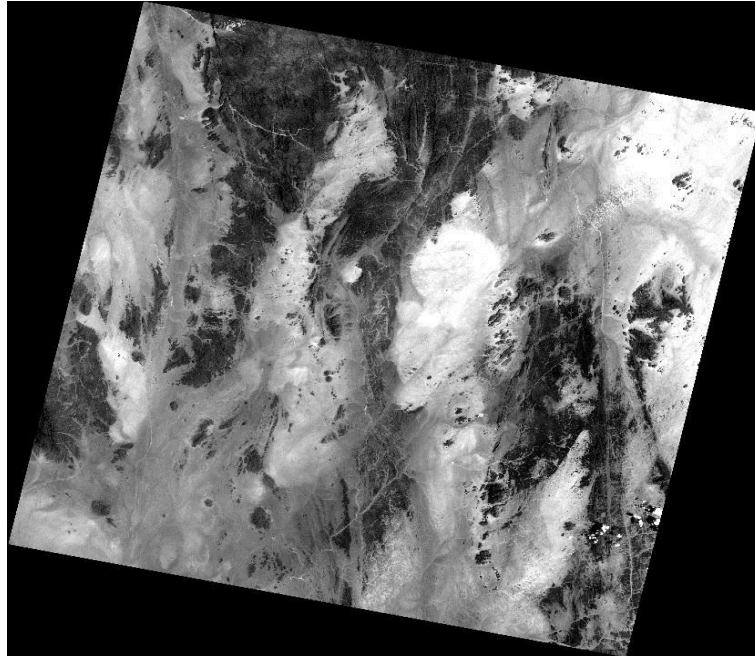


Figure: satellite image of tesnou

SPACECRAFT_ID = "LANDSAT_8" has 11 bands and ends with file header group one of projection group using meter as a unit and "WGS84" as an ellipsoid.

TABLE I. LANDSAT 8 OLI MULTI-SPECTRAL BANDS

Landsat 8 OLI Bands	Wavelength (micrometers)	Resolution (meters)
Band 1 - Ultra Blue (coastal/aerosol)	0.435 - 0.451	30
Band 2 - Blue	0.452 - 0.512	30
Band 3 - Green	0.533 - 0.590	30
Band 4 - Red	0.636 - 0.673	30
Band 5 - Near Infrared (NIR)	0.851 - 0.879	30
Band 6 - Shortwave Infrared (SWIR) 1	1.566 - 1.651	30
Band 7 - Shortwave Infrared (SWIR) 2	2.107 - 2.294	30
Band 8 - Panchromatic	0.503 - 0.676	15
Band 9 - Cirrus	1.363 - 1.384	30
Band 10 - Thermal Infrared (TIRS) 1	10.60 - 11.19	100 * (30)
Band 11 - Thermal Infrared (TIRS) 2	11.50 - 12.51	100 * (30)

Table 1: Band characteristics of "LANDSAT_8 OLI

1.2. Geoscientific data:

The study is also based on a large number of geoscientific data, namely the geological map of the el hoggar and tesnou region and several academic works (theses and research articles) these data were used as the ground truth in the lenement identification and the results obtained.

2/Software:

To reach the required results, we used two software to process the data from which our study Will be launched, SNAP, ENVI, which we will be as follows:

2.1. SNAP system:

SNAP, short for (Sentinel Application Platform) is an open source software developed by ESA (European Spatial Agency) for the scientific exploitation of Earth observation missions, With in the framework of the SEOM (Scientific Exploitation of Operational Missions) Programme. The SNAP structure is ideal for processing and analyzing Earth observation (EO) due to the following technological innovations: scalability, portability, standard rich client platform, general EO data stripping, tiled memory management, and chart processing framework. That made the Sentinel application platform a common structure for all Sentinel tool boxes. It was developed by Brockmann Consult, Skywatch, Sensar and C-S.(ESA, 2022) SNAP provides a common structure for all Sentinel toolboxes, as well as toolboxes for processing data from other satellite sensors. It represents the common architecture of the ESA

1/2/3 Sentinel Mission toolboxes, namely: S1TBX, S2TBX and S3TBX (contained by default in the SNAP software).

The various toolboxes implemented for SNAP not only allow opening, visualizing and Exporting satellite data, but also allow users to apply different levels of processing, from simple è-Data preprocessing steps to very advanced processing chains, set up (and executed in batches) via Graph Builder tool) can become. Note that SNAP is not limited to Copernicus satellite data, but can also process data from other EO satellites as well as from general and vector point data formats. SNAP functionality can be extended through plugins that can be browsed and installed from the user interface. Advanced users are encouraged to develop their own plugins. The platform also allows data to be browsed and downloaded directly from ESA SciHub through a built-in product library that also provides simple filtering tools and zone identification as an Open Hub web interface (CSEOL).Because we do not master this software, our use is limited to the pre-processing of Sentinel 2A data that can not be performed under any other software.

2.3. Surfer system:

Surfer is a full-featured 2D and 3D drafting, modeling and analysis package for scientists and engineers. Surfer's sophisticated interpolation engine quickly converts XYZ data into publication-quality maps. Almost every aspect of the map is customizable. Enhance maps with profiles, legends, titles and labels, faults and breaklines, or external maps from any web mapping service Surfer is widely used by geologists, geophysicists, hydrologists,

archaeologists, oceanographers, biologists, consultants, engineers and many others around the world

II. Methodology:

Our study is based on main studies, which is linear and, but before starting our study we will touch on a step called Image preprocessing.

The use of these satellites images requires a process called “atmospheric correction” (QuangTu Bui et al., 2022). This process aims to remove the contribution of the atmosphere from the total top of atmosphere reflectance measured by the remote sensors.

The Rayleigh Scattering Correction processing can only be performed for landsat 8-1Lc data, because 1Lc data is not atmospheric corrected yet. This processing is organized in several steps. First the Rayleigh reflectance is computed for every 4x4 pixels window. Then, Rayleigh transmittance and Rayleigh spherical albedo are computed for every 4x4 pixels window. Then, the TOA apparent reflectance corrected for gaseous absorption ρ_{ng} is corrected for Rayleigh contributions for each pixel in order to derive the top of aerosol reflectance ρ_{top} . The 4x4 pixels windows do not overlap.

1. The Rayleigh Correction algorithm has originally been designed for MERIS, but is Basically not sensor-dependent. The current SNAP processor version also supports OLCI and landsat8 instruments.

Landsat 8 satellite images needs to be corrected where we changed the proposed settings in the SNAP program.

1.2.1. Processing Parameters

Source bands: The bands in the L1b source product. Select the spectral bands to be Rayleigh Corrected. Multiple selection is possible. With this processor, the spectral bands 1-15 for MERIS, 1-21 for OLCI, and 1-9 for S2 MSI can be Rayleigh corrected.

Compute Rayleigh optical thickness bands: Rayleigh optical thickness bands are generated and written to the target product. Default value is false.

and written to the target product. Default value is false.

Compute bottom of Rayleigh reflectance bands: Bottom of Rayleigh reflectance ('Rayleigh-corrected') bands are generated and written to the target product. Default value is true.

Compute gaseous absorption corrected TOA reflectance bands: Gaseous absorption corrected TOA reflectance bands are generated and written to the target product. Default value is false.

Compute TOA reflectance bands: TOA reflectance bands are generated and written to the target product. Default value is false.

Add air mass: Air mass term is generated and written to the target product. Default value is false.

Image resolution in m in target product (S2 MSI only): The unique image resolution in the target product. Applies for S2 MSI input products only. Source bands having a different resolution are rescaled properly before being Rayleigh corrected. Default value is 20m.

Sea level pressure in hPa (S2 MSI only): Constant sea level pressure in hPa. Applies for S2 MSI input products only. For OLCI and MERIS this information is available from the tie point grids. Default value is 1013.25 hPa, we calibrated to 1011,25 hPa from the Sea level Pressure Map of August 2018 (Fig. 26) downloaded from the IRI Data website (International Research Institute Data).

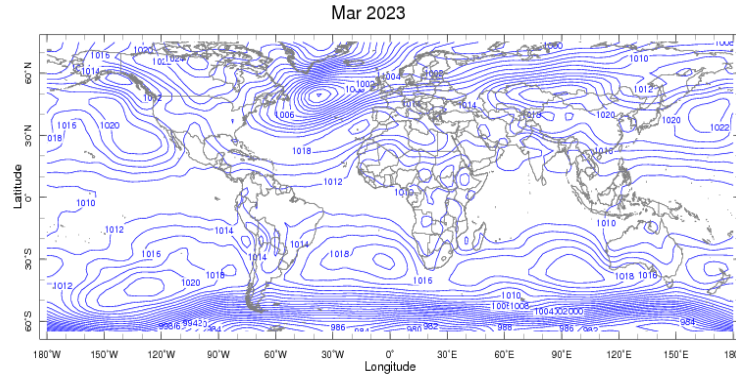


Figure: sea level pressure on March 2023

Ozone in DU (S2 MSI only): Constant ozone value in DU. Applies for S2 MSI input products only. Default value is 300 DU

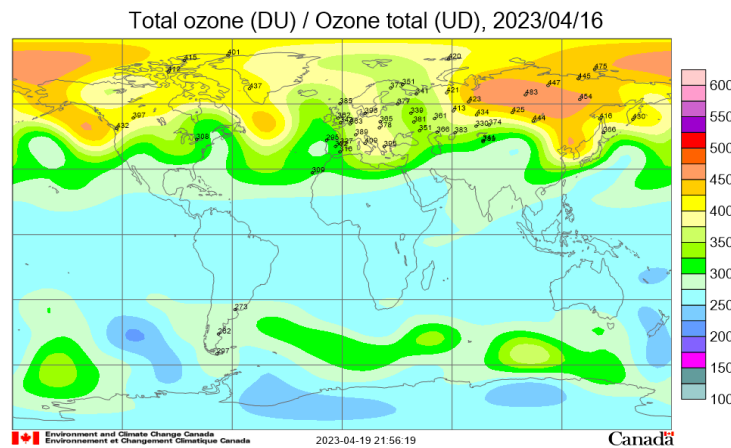


Figure: for ozone in DU

2.1.1. Color composition:

Color composition is a visual characterization of the analysis and interpretation of lithology of the area studied through satellite imagery that allows to distinguish the spatial division of the area by combining three RGB colors of spectral composition. In our study area, we have a spectral range of several spectrums for a clear structure to complete our treatment, but we found that there are several good combinations for each configuration to show an advantage that the other does not have. We also reduced scales 1 and 2, because on the day the images were taken, the spectrums mentioned were not acceptable in the climate to Atmospheric correction (HASSANI, 2017)

Correlations Bande 7	Bande5	Bande 4	Bande 3	Bande 2	Bande 1	
Bande 7	1	0,979179	0,94299	0,85921	0,89741	0,779638
Bande 5	0,979179	1	0,961893	0,88096	0,917749	0,79453
Bande 4	0,94299	0,961893	1	0,919252	0,969075	0,87369
Bande 3	0,859213	0,88096	0,919252	1	0,915982	0,807559
Bande 2	0,897414	0,917749	0,969075	0,915982	1	0,911547
Bande1	0,779638	0,79453	0,87369	0,807559	0,911547	1

Table: Correlations between bands

Through this table of band correlation and several attempts we extract the effective color composition that gives us different information about the study area .

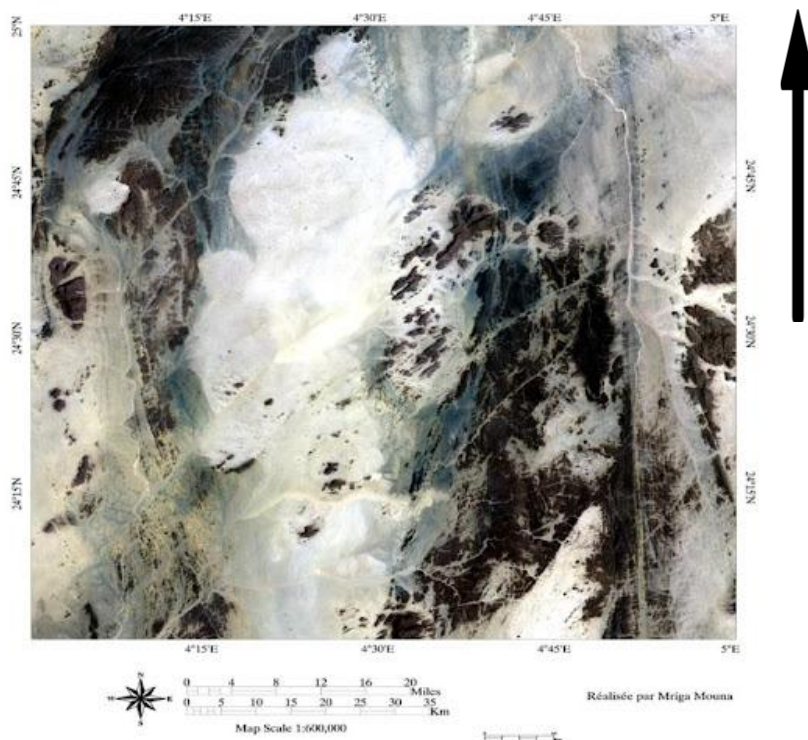


Figure: tesnou coordinates using colored composition



Figure: colored compositin (R7 G5 B1)

2.2. Thematic treatment:

2.2.1. Transformation treatments:

The most commonly used among image transformation processes are Analysis in principal components (ACP), ratios and filtering..... (Hammad, 2008)

All three treatments were applied. The ratios are particularly interesting because they generate new images by combining the different sources of information to enhance some of the data properties that are less visible in the original image. The neocanals, often of better quality, constitute an excellent visual interpretation product. Filtering on the other hand allows the detection of textural limits so we reserve them linear mapping .(Hammad, 2008)

a.Principal component analysis (PCA):

Principal Component Analysis is an effective technique for enhancing an image for geological interpretation purposes. It reduces the information contained in several bands, highly correlated into a limited number of components, Sometimes the information in 5 or 6 bands is reduced by this analysis in only 3 components. Choosing the number of main components to keep is the most important step of the CPA. No general rule of decision being defined, the user is free retain the desired components according to criteria specific to their study the main component analysis thus produces new channels. These create colourful compositions that are an excellent product visual interpretation, thus increasing the contrast between the various objects on the ground (Hammad, 2016).

A.1.Advantages of PCA:

PCA has many advantages, which are described below:

- Principal Component Analysis (PCA): PCA is an effective technique for emphasizing a multispectral image for purposes of geological interpretation. It makes it possible to reduce the information contained in several bands, highly correlated, into a small number of components (Coulibaly, 1996).

The principal component analysis thus produces new channels. These make it possible to create colorful compositions that constitute an excellent product of visual interpretation, thus increasing the contrast between the various objects on the ground.

PCA, pixel contrast appears in one or two components, which are two principal components and are usually the maximum information carrier, and it is possible to cast room for another group.

- Work from decorative strips (zero correlation) to ensure there is no redundancy between data.

- Transformation can be useful for separating objects by maximizing contrast by highlighting radioactive details of objects. (Hammad, 2016)

in our study we relied on the graphic curve to select the effective bands in pc

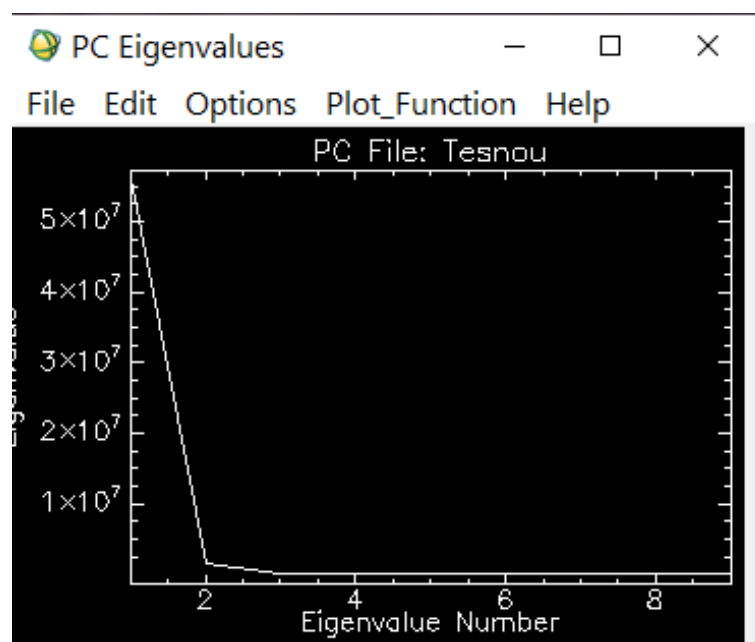


FIGURE: PC FILE OF TESNOU

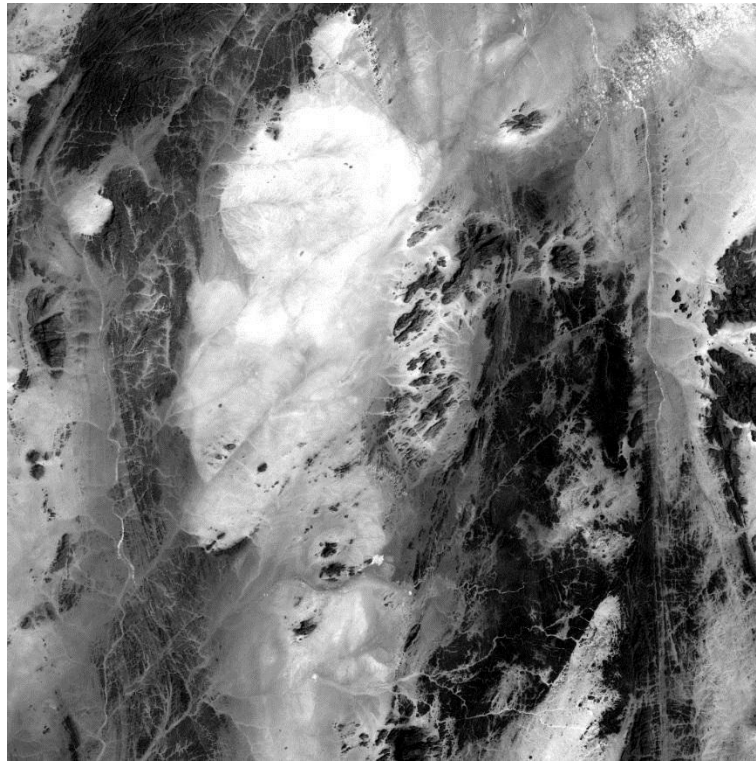


Figure: CP 1

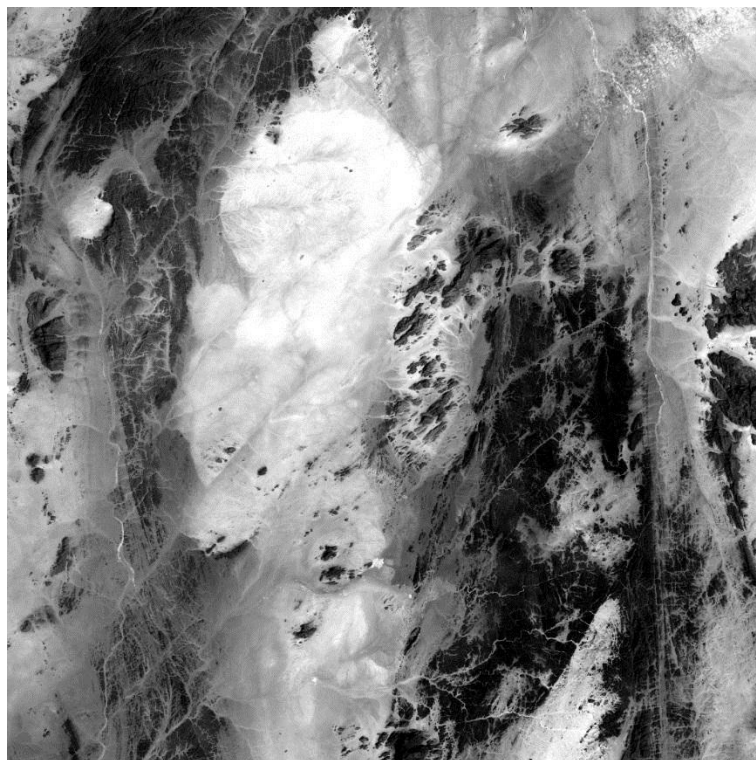


Figure: CP 2

● **b. band Ratio:**

This analysis is based on the concept of reflection, the power-to-energy ratio Energy reflected by the body and received by the sensor. This method can Reduce the effect of terrain

and increase the contrast between metallic surfaces. The practice is to identify the bands (pairs) used to calculate the ratio. The ratio bands corresponds to a new channel whose pixel value is equal to the ratio of the radiation values of the two initial channels. This novel ratio image can overcome differences in illumination and pixel separation, where additional information is obtained (Hammad, 2016).

2.2.2. Spatial filtering of images:

Spatial filters are local operators that, according to Caloz and Collet (2001), take into account the neighborhood of a signal element, pixels in an image processing, to distinguish, attenuate, or extract a local property such as gradient, average, or other statistical parameters. So that the application of these factors helps in increasing the clarity of the image so that the border lines appear more clearly while preserving the necessary amount of information. In other words, edges are detected and optimized within spatial units so that several spatial filter operators are distinguished according to the purpose of each Application.

Table 4: Spatial filter operators : The table shows the main types

Function	Convolution operator	Operator statistical	Morphological operator
Smoothing (low pass)	Simple moving average	Medium	Erosion
	Weighted Moving Average	Median	Dilation
		Mode	Opening
Enhancement local (high pass)	Omnidirectional	Amplitude	gradient
	gradient	Standard	morphological
	(Laplacian)	deviation	top hat
	Directional	Quantil	Valley bottom

To confirm regions with abrupt differences in intensity (Kouamé, et al., 1999), highfrequency type filters are specifically designed to detect and optimize Describe it to emphasize This difference. The software with which we perform our processing, ENVI 4.5, performs several types of filtering operations: convolution filters, morphological filters, adaptive filters and filters by Fourier transform (FFT).

By highlighting and launching the corresponding features of stone or structural interruptions, we selected the directional filter.

a.Directionnal filter:

The first derivative of an image is an edge enhancement filter, which selectively enhances the features of an image that contain specific directional components

The sum of the elements of the directional filter kernel is zero. This causes areas of the output image with uniform pixel values to be zeroed out and variables to appear as sharp edges.

These directional filters visually enhance the shadows cast on the image as if illuminated by grazing light (Marion, 1987).

Furthermore, this type of filter can improve lines that the light source does not like (Drury, 1986). Under ENVI, the line is strengthened in all directions. At an angle of 45°, all possible orientations are possible, and the size of the filter differs from its effect along the optimization line, identifying structures larger than or equal to, while smaller structures blend into the image noise (Collwell, 1999). 1983; Kwame et al, 1999). Several authors such as Hornsby and Bruce (1985) A 5 × 5 filter is retained on the image, the resolution of which is based on structural studies at the regional level. As part of our study and considering the size of the study area, we chose a 5×5 mainline window and a 3×3 window as the fine structure. These filters are raw bands (ETM 3, ETM5 (ETM+3/ETM+4, ETM+4/ETM+7) It should be noted that 5-band filtering allows authors to view.(Hammad, 2016).

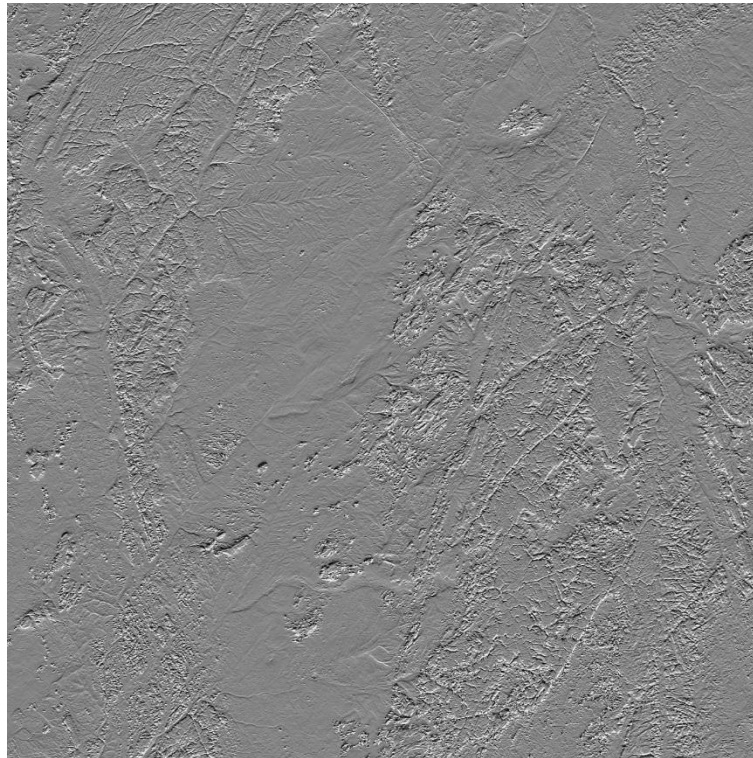
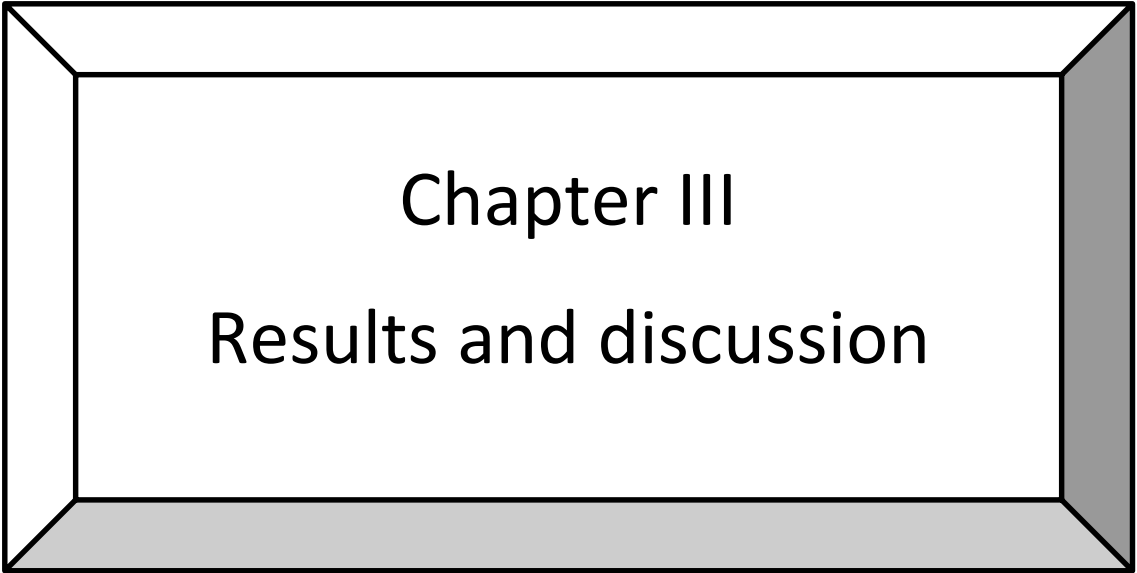


**Figure: directional filter on (R8 G6 B4) at 90° with 5x5 Kernel
Extraction of lineament**

All of our previous operations are to prepare the lener map using Surfer software. And that's by putting the images of directional filter and the geological map on top of some of them and drawing lines



. Figure: extraction Map of the lineaments using DF 135° M 7x7 and geological map



Chapter III

Results and discussion

I. Results

1. Results of satellite image interpretation analysis

Through remote sensing, surfer software and photo observation, we have reached the following results

1.1.1. Colored composition using Landsat 8 (R7 G3 B2)

For this composition, the prominent lithological unit component is green, deep red and color gradient is well visible in the same colors but light plus white. Which enabled us to know the places with similar lithological units in terms in type .

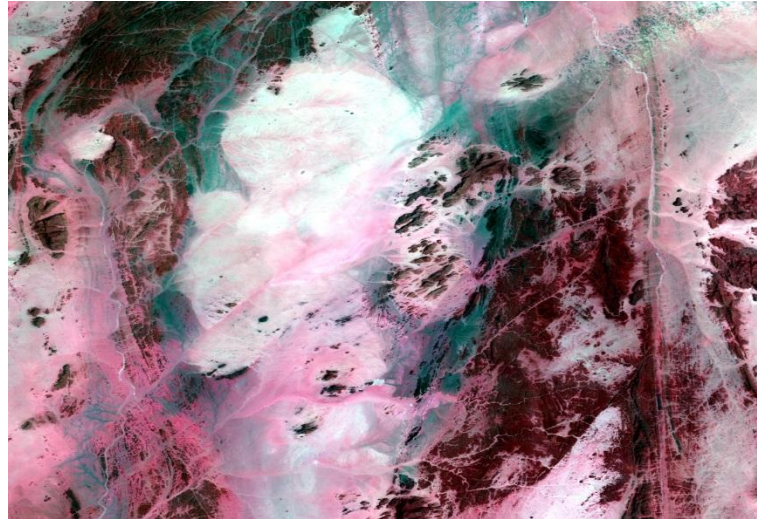


Figure: Colored composition (R7 G3 B2)

1.1.2. Colored composition Results (R7 G6 B1)

One of the best Colored composition obtained in our study, that we confirmed the results of the Previous Figure, as well as the demonstration of some geological forms that did not appear before with this precision.

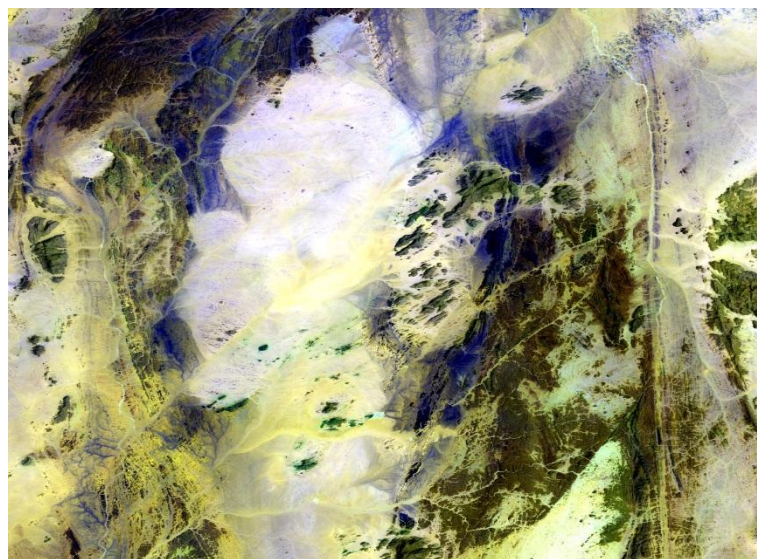


Figure: Colored composition (R7 G6 B1)

1.2. Enhanced Filter Result:

We used this filter to increase brightness on the image as we applied it over the three Band (R8 G6 B1) which helped us to differentiate geological spaces, fractures and folds As the figure below shows.



Figure: Enhanced filter on LANDSAT OLI 861 in RGB

1.3. Principal Component Analysis Result (PCA):

Due to this composition of ACP we get an exact analysis of the lines through the distribution of yellow, orange and pink colors and the appearance of the lines in a different color which made them clear and visible and easily discernible thickness

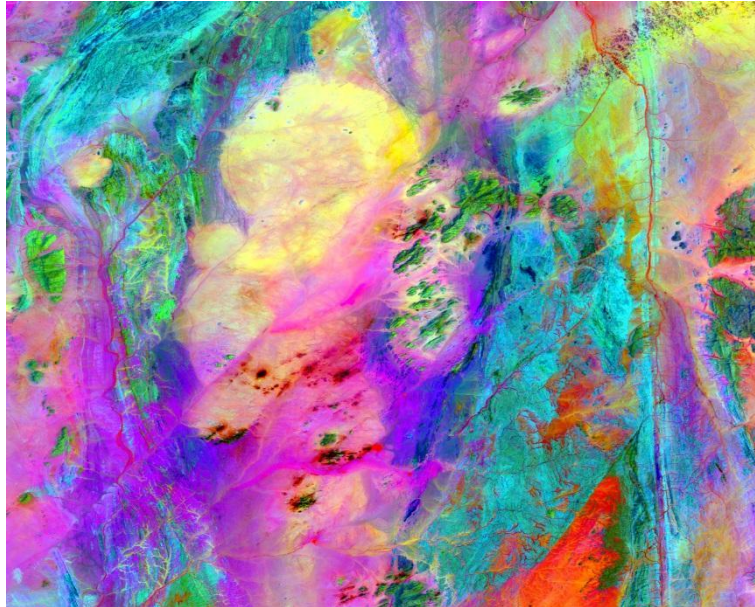


Figure: Colored composition using PCA (RCP3 GCP2 BCP1)

1.4. Band Ratio Result

In this case, we did a different process, a color combination between the normal band and band ratio, which gave us a great result in showing fine lines and making them more clear

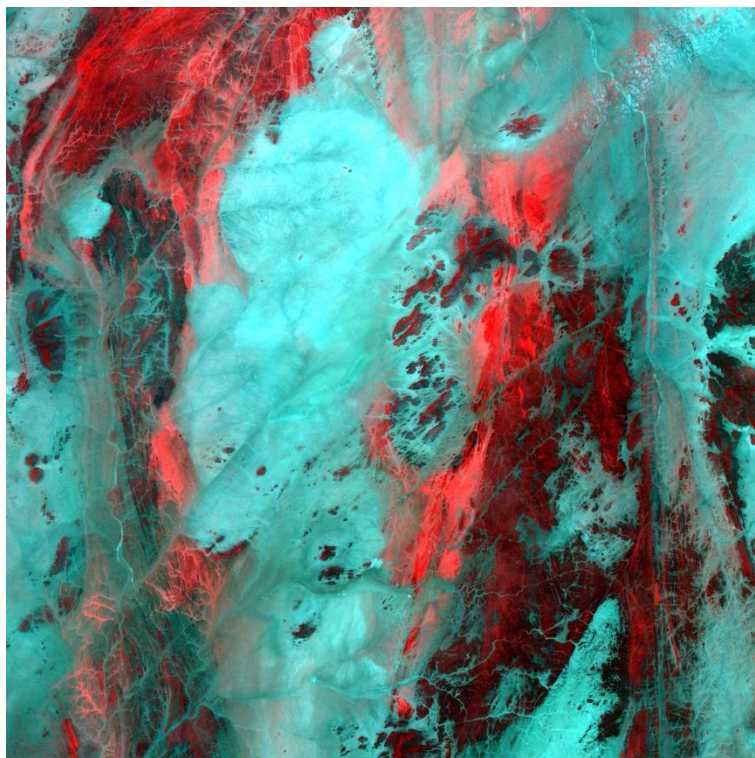


Figure : Colored composition using band ratio (R8/6 G2 B1)

2. Lineament Mapping .

2.1. Filtering Treatment Results:

For Earth observation data from landsat 8 satellites most of the information is in Band 2 so we chose to apply filtering to this first major component. To characterize the tectonic formations affecting the topography of the study area, we used the directional filter by enhancing several angles (0°, 45°, 90°, 135°...etc) and we found that the best angle shows everything. Tectonic changes at 135° angle The 7x7 deflection window was found to be the most suitable for our study as it allows to see full structural details. Because The main goal of applying directional filters is to detect any linear shape (contours, fractures and defects) in order to reduce blurring and smoothness of the image

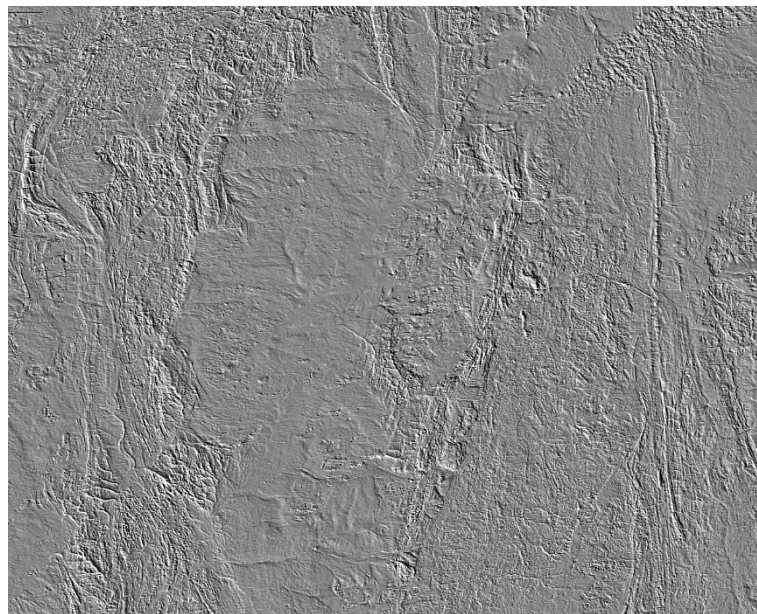


Figure: Directional Filter 135 ° with 7x7 Matrix.

2.2. Results of manual line extraction:

Manual extraction performed after good knowledge of the Earth, allowed us to remember that linear charts are considered structural (defects, folds, etc.) plus that Geological nature is clear on land such as our study area, Contains circular geological forms Manual extraction of linear lines by interpreting images more effectively when analyzing structures and General understanding of the image We imported images from the processing of the filter we converted to Surfer to map the lines that appear very clearly. Although this analysis is slow and cumbersome, we have come to a satisfactory conclusion so that when you put the line map over the geological map, there is complete integration between them.

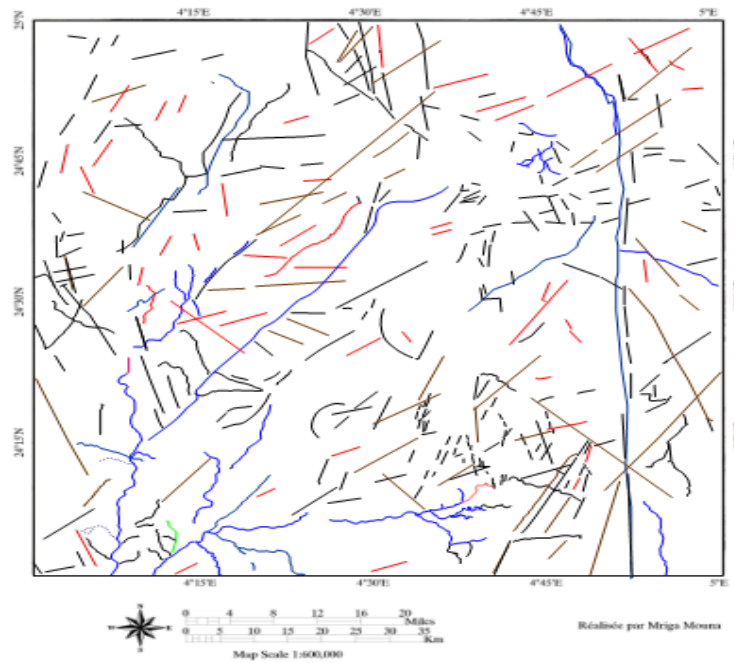


Figure 39: Map of the lineaments extracted using DF 135° M 7x7 and geological map

Automatic extraction of lineaments

The automatic lineament extraction process in the study utilized the PCI Geomatica 2016 software. User-defined parameters were crucial for the extraction process. The approach followed the methodology involved applying the process to each of the four images of directional filters at different orientations (N0°, N45°, N90°, and N135°). Additionally, Principal Component Analysis (PCA) was performed on the 7x7 matrix directional filters using the ENVI software.

Numerous detection algorithms have been employed to automate lineament extraction from remotely sensed images (Hammad et al., 2016). The automatic extraction of lineaments was accomplished using the Line tool in the Geomatica software. This tool is specifically designed to extract linear features from images. The figure below shows the lineaments extracted automatically by the algorithm LINE of PCI Geomatica 2016.

The number and the shape of the lineaments extract is very different compared to those traced manually. We can note that the submeridian direction is dominating in this case.

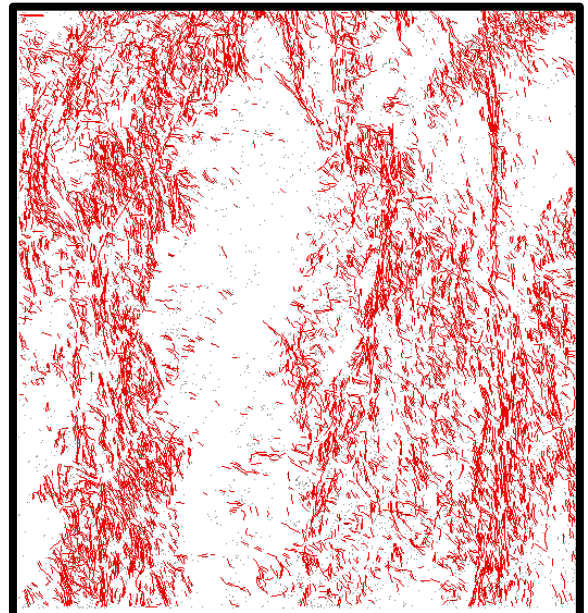
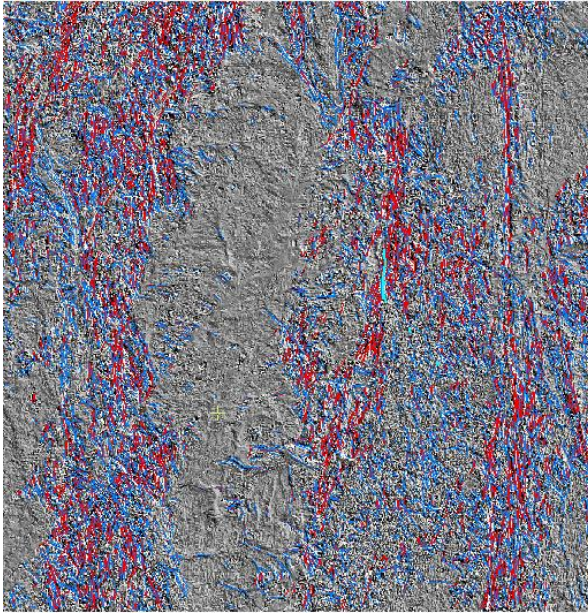


Figure 39: Extraction automatic

II. Discussion

After referring the results obtained through all the processes carried out in the area studied during this work, we reached an excellent match between the geological map and remote sensing images, which made it easier for us to draw the linear map and the appearance of lines that might represent (faults and cracks), and confirmed the consistency of some units and confirmed the asymmetry of others by appearing in different colors compared to the classification on the map.

Due to the image of the directional filter, and the excellent quality of the remote sensing images, the map of the lines that are considered new contribution and updates to the geology of the region was completed especially in terms of linear geological forms

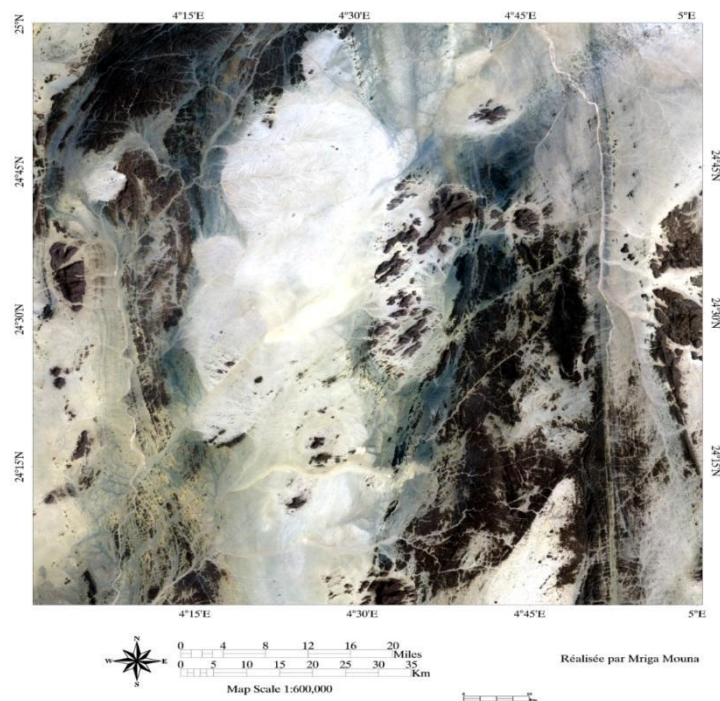


Figure: tesnou coordinates using colored composition



General conclusion

General conclusion

The manual extraction of lineaments is considered a very important and positive method in geological studies. This technique of lineament extraction serves to reduce the time spent on field missions, and also has informational importance from the geodynamic point of view, and the tectonic heritage of the study area. This work is based on the Landsat 8 OLI, which is commonly used in this type of study because of its spectral potential and its spatial extension. Through processes we have discovered new lines to other lines that were present in the geological map. This introduction of remote sensing in mapping in this way allows an effective and accurate definition of lines and speed in detecting cracked areas



Bibliography

Bibliography

1. **ALLAOUI M., BELBALI S. 2013.** Signification de la presence de la tourmaline dans les Filons aurifere, l'interet pour la prospection des Gisements. Exemple de l'indice assouf mellene feuille Tesnou terrane d'iskel, hoggar occidentals. Master Mem. Aboubaker Belkaïed University, Tlemcen.
2. **Azzouni-Sekkal, A., Liégeois, J-P, Bechiri- Benmerzoug, F., Belaïdi-Zinet, S., Bonin, B., 2003.** The "Taourirt" magmatic province, a marker of the closing stage of the Pan-African orogeny in the Tuareg Shield: review of available data and Sr- Nd isotope evidence. *Journal of African Earth Sciences* 37, 331-350.
3. **Bertrand, J. M. L., Caby, R., 1978.** Geodynamic evolution of the Pan-african orogenic belt: a new interpretation of the Hoggar shield. *Geologische Rundschau* 67, 2, 357-388.
4. **Black, R., Latouche, L., Liégeois, J-P. , Caby, R., Bertrand, J-M., 1994.** Pan-African displaced terranes in the Tuareg shield (central Sahara). *Geology* 22, 641- 644.
5. **Blinikov, V., 1987-1990. Blinikov, V et Popov, V., 1991. Rapports** sur les résultats des travaux de recherche systématiques et les levés géologiques à l'échelle 1/200000 sur les feuilles Tesnou et Iftesséne. Rapport inédit ORGM, Boumerdés, 322 p.
6. **Caby, R., Andreopoulos-Renaud, U., and Gravelle, M., 1982.** Cadre géologique et géochronologique U/Pb sur zircon des batholites précoces dans le segment panafricain du Hoggar central (Algérie). *Bull. Société Géologique de France*. Vol. 24, p 677- 684.
7. **farah Abdelouahed, Algouti Ahmed, Mohammed Ifkirne, Mohamed Ait Mlouk,2022,** Lineament mapping in the Central High Atlas using ASTER and ASTER-GDEM data, (Morocco), *Boletin de la Sociedad Geologica Mexicana*.
8. **Farah Abdelouhed1,, Ahmed Algouti1, Abdellah Algouti1. Mohamed Ait Mlouk1, and Mohammed ifkirne 2020** Lithological mapping using Landsat 8 Oli multispectral data in Boumalne, Imider, and Sidi Ali Oubork, High Central Atlas, Morocco, Cadi Ayyad University, Faculty of Sciences, Department of Geology, Geosciences, Geotourism, Natural Hazards and Remote Sensing Laboratory. Bd. BO 2390, 40000 Marrakech.
9. **Fati BOUBACAR,et Moussa KONATÉ 2020** UTILISATION DE LA TÉLÉDÉTECTION ET DU SIG POUR LA CARTOGRAPHIE DES ZONES MINÉRALISÉES EN OR DANS LA PROVINCE PANAFRICAINNE DU SUD EST NIGER (SUD MARADI ET DAMAGARAM-MOUNIO) Université Abdou Moumouni, Faculté des Sciences et Techniques, Département de Géologie, Laboratoire des Eaux Souterraines et des Géoressources, BP 10662 Niamey, Niger.
10. **Hammad Nabila, 2016.** Cartographie géologique et analyse linéamentaire de la région d'El Kseïbat (Sahara du sud-ouest) à partir des images spatiales. Incidence sur l'exploration minière.
11. Hammad Nabila, cour télédétection ,cartographie des linéaments géologique, Université kasdi merbah ouargla
12. **HAMMAD Nabila1, DJIDEL Mohammed1, MAABEDI Nawel1,** CARTOGRAPHIE DES LINEAMENTS GEOLOGIQUES EN DOMAINE ARIDE PAR EXTRACTION SEMI-AUTOMATIQUEARTICLE, Université Kasdi Merbah Ouargla, Laboratoire de Géologie du

- Sahara, Faculté des Hydrocarbures, des Energie Renouvelables et des Sciences de la Terre et de l'Univers, Ouargla 30 000 Algérie
13. **Hammad Nabila, 2008.** Apport de la teledetection a haute resolution a la discrimination lithologique en domaine semi desertique et aride : application a la region du djebel drissa (massif des eglab). Diplôme de magister
 14. <https://earth.esa.int/eogateway/tools/snap>
 15. **SAIDI MARIA 2022** Spatial repartition of Silurian and Frasnian Shales formations using Remote Sensing Data in Bled El Mass (Ahnet basin); master mem, KASDI MERBAH- OUARGLA UNIVERSITY FACULTY OF HYDROCARBONS, RENEWABLE ENERGIES AND EARTH AND U8. <https://www.geo.university/courses/tutorial-to-esa-snap-software>
 15. <https://www.coursegeologie.com>
 16. <https://www.g2.com/products/surfer/review>
 17. <https://www.geo.university/courses/tutorial-to-esa-snap-software>
 18. **Liégeois, J.P, Latouche, L., Navez, J., Black, R., 2000.** Pan-African collision, collapse and escape tectonics in the Tuareg Shield: relations with the East Saharan Ghost Craton and the West African Craton. In: Wallbrecher, E., Loizenbauer, J., Fritz, H., Unzog, W., Mogessie, A., (Eds.), Special abstract issue, 18th Colloquium of African Geology, Graz. Journal of African Earth Sciences 30/4A, Elsevier, pp. 53-54.
 19. **Liégeois, J.P., Latouche, L., Boughrara, M., Navez, J., Guiraud, M., 2003.** The LATEA metacraton (Central Hoggar, Tuareg Shield, Algeria): behaviour of an old passive margin during the Pan-African orogeny. Journal of Earth Sciences 37, 161-190.
 20. **Meryem Redouane, Faouziya Haissen, Hicham Si Mhamdi , Mohammed Raji.2022** L Article in Open Journal of Geology ineaments Extraction and Analysis Using Landsat 8 (OLI/TIRS) in the Northeast of Morocco.
 21. **moujane said, Ahmed Algouti, Abdellah Algouti, Abdelouahd Farah,2022,** Mapping lineaments using Landsat 8 OLI and SRTM in the Boumalne-lmiter regions of the southernCentral High Atlas. Morocco, This work is licensed under a Creative Commons Attribution 4.0 International License.
 22. **Zhiqi Yu, Liping Di, Ruixing Yang, Junmei Tang, Li Lin, Chen Zhang, Md. Shahinoor Rahman, Haoteng Zhao, Juozas Gaigalas, Eugene Genong Yu, Ziheng Sun,2019** Selection of Landsat 8 OLI Band Combinations for Land Use and Land Cover . Center for Spatial Information Science and Systems, George Mason University, Fairfax, VA, USA.